AFRL-RX-WP-TP-2008-4329

USING DEFORMATION MODES TO IDENTIFY CRACKS IN TURBINE ENGINE COMPRESSOR DISKS (PREPRINT)

Robert A. Brockman, Reji John, and Marc A. Huelsman

Metals Branch
Metals, Ceramics, and NDE Division

OCTOBER 2008

Approved for public release; distribution unlimited.

See additional restrictions described on inside pages

STINFO COPY

AIR FORCE RESEARCH LABORATORY
MATERIALS AND MANUFACTURING DIRECTORATE
WRIGHT-PATTERSON AIR FORCE BASE, OH 45433-7750
AIR FORCE MATERIEL COMMAND
UNITED STATES AIR FORCE

REPORT DOCUMENTATION PAGE

Form Approved
OMB No. 0704-0188

1. REPORT DATE *(DD-MM-YY)*
October 2008

2. REPORT TYPE
Journal Article Preprint

3. DATES COVERED *(From - To)*

4. TITLE AND SUBTITLE
USING DEFORMATION MODES TO IDENTIFY CRACKS IN TURBINE ENGINE COMPRESSOR DISKS (PREPRINT)

5a. CONTRACT NUMBER
In-house

5b. GRANT NUMBER

5c. PROGRAM ELEMENT NUMBER
62102F

6. AUTHOR(S)
Robert A. Brockman and Marc A. Huelsman (University of Dayton Research Institute)
Reji John (AFRL/RXLMN)

5d. PROJECT NUMBER
4347

5e. TASK NUMBER
RG

5f. WORK UNIT NUMBER
M02R3000

7. PERFORMING ORGANIZATION NAME(S) AND ADDRESS(ES)

University of Dayton Research Institute

Metals Branch (AFRL/RXLMN)
Metals, Ceramics, and NDE Division
Materials and Manufacturing Directorate
Wright-Patterson Air Force Base, OH 45433-7750
Air Force Materiel Command, United States Air Force

8. PERFORMING ORGANIZATION REPORT NUMBER
AFRL-RX-WP-TP-2008-4329

9. SPONSORING/MONITORING AGENCY NAME(S) AND ADDRESS(ES)
Air Force Research Laboratory
Materials and Manufacturing Directorate
Wright-Patterson Air Force Base, OH 45433-7750
Air Force Materiel Command
United States Air Force

10. SPONSORING/MONITORING AGENCY ACRONYM(S)
AFRL/RXLMN

11. SPONSORING/MONITORING AGENCY REPORT NUMBER(S)
AFRL-RX-WP-TP-2008-4329

12. DISTRIBUTION/AVAILABILITY STATEMENT
Approved for public release; distribution unlimited.

13. SUPPLEMENTARY NOTES
Journal article submitted to The Aeronautical Journal, published by the Royal Aeronautical Society.

PAO Case Number: 88ABW 2008-0705; Clearance Date: 28 Oct 2008. The U.S. Government is joint author of this work and has the right to use, modify, reproduce, release, perform, display, or disclose the work. Paper contains color.

14. ABSTRACT
Recent studies show that analytical predictions of crack growth in rotating components can be used in conjunction with displacement measurement techniques to identify critical levels of fatigue damage. However, investigations of this type traditionally have focused on the detection of damage at known flaw locations. This paper addresses the related problem of estimating damage associated with flaws at unknown locations, through the combined use of analytical models and measured vibration signatures. Because the measured data are insufficient to identify a unique solution for the location and severity of fatigue cracks, the function of the analytical model is to bound the extent of damage occurring at life-limiting locations. The prediction of remaining life based on estimates of worst-case damage and crack locations also is discussed.

15. SUBJECT TERMS
deformation, fatigue crack, turbine engine, compressor disks, fatigue damage, life prediction

16. SECURITY CLASSIFICATION OF:			17. LIMITATION OF ABSTRACT:	18. NUMBER OF PAGES	19a. NAME OF RESPONSIBLE PERSON (Monitor)
a. REPORT	b. ABSTRACT	c. THIS PAGE			James M. Larsen
Unclassified	Unclassified	Unclassified	SAR	34	19b. TELEPHONE NUMBER *(Include Area Code)* N/A

Standard Form 298 (Rev. 8-98)
Prescribed by ANSI Std. Z39-18

USING DEFORMATION MODES TO IDENTIFY CRACKS IN TURBINE ENGINE COMPRESSOR DISKS

Robert A. Brockman[1], Reji John, and Marc A. Huelsman[1],

U.S. Air Force Research Laboratory, Materials and Manufacturing Directorate, AFRL/RXLMN,
Wright-Patterson Air Force Base, OH 45433 USA

[1]University of Dayton Research Institute, 300 College Park, Dayton, OH 45469 USA

Abstract

Recent studies show that analytical predictions of crack growth in rotating components can be used in conjunction with displacement measurement techniques to identify critical levels of fatigue damage. However, investigations of this type traditionally have focused on the detection of damage at known flaw locations. This paper addresses the related problem of estimating damage associated with flaws at unknown locations, through the combined use of analytical models and measured vibration signatures. Because the measured data are insufficient to identify a unique solution for the location and severity of fatigue cracks, the function of the analytical model is to bound the extent of damage occurring at life-limiting locations. The prediction of remaining life based on estimates of worst-case damage and crack locations also is discussed.

1. Introduction

One of the more attractive applications of material prognosis technology is the life management of turbine engine disks, which are expensive to replace, difficult to inspect, and operate in complex and hostile loading environments that dictate a highly conservative retirement philosophy. The ability to monitor the damage state of such components, project subsequent damage development, and estimate remaining life would be revolutionary in terms of cost savings, safety, and fleet readiness.(1-3)

Recent experimental investigations(4,5) suggest that the prospects for damage detection in rotating components are significantly improved by averaging measured responses over a large number of cycles, and by signature monitoring based on prior knowledge of the damage modes of interest. In what follows, we discuss the use of analytical models to provide accurate information for use

in the pattern recognition process leading to damage detection. The study uses an idealized compressor disk model in which known damage states can be introduced to generate baseline signatures for probable damage modes. The same disk model is used here to simulate the measured data for a system containing one or more cracks whose size and location are not known *a priori*. Both the accuracy and the conservative or non-conservative nature of the predictions are of interest.

It should be noted that significant questions exist about the feasibility of performing adequate displacement measurements in such systems. This paper does not address measurement issues; however, experimental investigations now in progress will, we hope, provide further guidance on sensor requirements and other practical issues.

2. Rotor Crack Detection

Monitoring of structural integrity is an area of broad interest, encompassing civil structures,(6,7) aerospace vehicle structures,(8,9) and engine systems for power generation and propulsion.(4,10) Each of these areas provides unique challenges in terms of instrumentation, data collection, pattern recognition, and analytical modeling. The most significant progress has been made in structural health monitoring of aerospace and civil structures, in which it is often feasible to employ numerous sensors, and the process of data collection and analysis is in many respects straightforward. Turbine engines present particularly difficult challenges in health monitoring, since the thermal environment is hostile, the components of interest are mostly rotating, and the flow path must remain unobstructed. For this reason, most engine health monitoring efforts have been limited to the detection or monitoring of cracking in shafts.(11-13)

The potential benefits of a reliable methodology for monitoring turbine engine structures are enormous, given the replacement cost of bladed disks designed for high-temperature, high-stress service conditions. Presently, developments in engine health monitoring are of greatest interest to defense customers, to minimize sustainment costs; however, the prospect of selling “power by the hour” to commercial customers may soon provide equally great incentives to the propulsion industry.

Certainly the most significant challenges in engine health monitoring are logistical, since the environment inside a turbine engine places severe limitations on the number and type of sensors that might be used. However, some possibilities do exist, in the form of temperature probes,

blade-tip clearance or arrival time measurements from capacitive probes, and magnetostrictive gauges attached to the shaft or other lower-temperature surfaces. Ground-based measurements conducted between flights, and off-wing measurements performed during maintenance work, may be used to augment the dynamic measurements made in service. Recent experiments on actual turbine disk hardware confirm that it is indeed feasible to detect and identify increasing damage using a combination of indirect measurements and analytical models, at least in the context of full-scale spin pit experiments (c.f. Figure 5 of Ref. 4).

In what follows, we use a model of an idealized compressor stage to demonstrate a process for identifying damage in the disk, bounding the likely crack size, and estimating key parameters such as the current stress intensity factor and fatigue crack growth rate. Our focus is on the analytical models needed to make the proper connections between remotely measured data and localized response at a probable damage site. Additional refinements are certainly possible in some areas, such as signal analysis and probability estimation.[14,15]

3. Disk Model

Our model of a generic engine disk possesses geometric, mass, and stiffness characteristics typical of a compressor disk, but is not based on a particular production component. In the present study, we simplify the model by representing the blades only by pressures in the slots, and monitoring displacement values in the blade posts. The disk has an inner radius of 80 mm, outer radius of 205 mm, and varies in thickness between 2.5 and 20 mm (Figure 1). The mechanical properties are typical of a Ni-base superalloy ($E = 200$ GPa, $\nu = 0.30$, $\rho = 8{,}300$ kg/m^3). Most of the results that follow correspond to a nominal rotation speed of 10,000 RPM.

The complete disk model consists of 24 nominally identical sectors, represented by copies of a single substructure spanning 15 degrees of arc (Figure 2). Each sector contains a single 10-mm hole in the web, and two blade slots.

To introduce a crack in any sector of the disk, we create a modified version of the basic substructure in which the crack is introduced. We have used the Zencrack[16] software to generate focused meshes with quarter-point finite elements surrounding the crack tip, as shown in Figure 3. The use of the detailed crack tip mesh allows the extraction of accurate stress intensity factor data in the cracked area(s).

A complete disk model containing a single crack consists of 23 identical uncracked substructures and a single cracked substructure. The external nodal connections in the cracked and uncracked sectors are identical; therefore, introducing one or more cracks is as simple as specifying a different substructure name to replace an uncracked sector. Multiple cracks located in separate sectors can be defined by identifying the appropriate (cracked) substructure models as needed. Multiple cracks, or variations in crack size, within a single sector require a new substructure definition, which becomes part of the component database and may be reused as needed. All analyses are performed using ABAQUS.[17]

4. Crack Signatures

Both "known" data (displacement signatures for cracks with known location and size) and "measured" data are generated in this study using the same library of substructures. However, our simulated "measured" data contain crack locations and sizes that are not represented in the baseline data. The "known" or baseline data represent analytical (or possibly measured) signature data generated for a particular component using existing design-analysis models, and stored in a component-specific database for later reference. The "measured" data represent field measurements collected in service or during routine maintenance.

Baseline crack signature data have been created for single cracks of various sizes in the disk bore, at the edge of the hole in the web, and in the base of a blade slot. The bore crack is elliptical, and located in the axial center of the bore. The hole and slot cracks are semicircular corner cracks. In each location, baseline crack signatures corresponding to crack lengths of 1.00, 2.25, and 3.50 mm have been predicted, providing a library of signatures for known damage types (Figure 4). In each case, the crack is located in the sector with one edge at an angular position of zero degrees. In all cases, the signatures characterizing damaged states of the disk consist of values of *displacement deviations*, or differences between the measured displacement and the steady-state value for the undamaged system.

Notice that the signatures for cracks in various locations are distinctive, in the sense that they each involve quite different combinations of displacement harmonic components. Note also that for the slot cracks, which are very near the sensor location, the peaks in the signatures are highly localized, while those further inboard exhibit more gradual amplitude variations. The amplitude of the signature for a given crack type varies nonlinearly with crack size. Corresponding to each

displacement signature in the library of known damage states, in addition to the crack size and location, is a value of the appropriate stress intensity factor for use in crack growth estimation. If a measured signature can be identified with a series of conditions in the database, it is possible not only to estimate a crack size, but also to interpolate for the corresponding stress intensity factor and (using the appropriate data for da/dN versus ΔK) the corresponding crack growth rate.

While the present disk model is highly idealized, the damage signature characteristics predicted by the model and used in the study are similar to those observed in fielded systems. Figure 5 shows typical signature data for a model of an actual bladed disk, for nominally-sized cracks in the bore and blade slot bottom. The slot crack signature for the idealized model exhibits somewhat more localized response than the actual system, but the character of the displacement patterns is quite reasonable.

It should be noted that several types of probes are commonly used for sensing blade tip position, based on capacitance, eddy current, and optical measurements. The probe may be positioned to give blade tip clearance in the radial or axial directions, or time of arrival. As such, it is possible to sense deflection patterns in terms of radial, circumferential, axial, or combined components of displacement. The choice of probe type, position and orientation is constrained by the geometry of the stage and the available space; in some situations, the magnitude of the displacements caused by blade vibration may overwhelm any evidence of damage elsewhere in the stage, dictating the use of a very specific sensor position and orientation. Figure 6 shows comparisons of signatures based on radial (clearance) and tangential (arrival time) displacement data for a single disk. Notice that the amplitude of each signature has been normalized using the steady state radial displacement. Two cycles of each trace are shown in the figure to make the patterns easier to discern. The displacement signatures for a particular damage location are distinctive, but the amplitudes and detailed character of the radial and tangential traces are different for each crack location.

5. Multiple-disk Systems

A word is in order regarding the magnitudes of the displacement deviations in the signature plots of Figures 4 through 6. While the displacement magnitudes are quite small, it should be noted that the data are obtained from a model of a single disk only, rather than of the complete rotor system. In a model of the disk alone, the asymmetry in response caused by the stiffness

perturbation in the cracked disk cannot be determined, since it depends on the mass and stiffness characteristics of the complete rotordynamic system. Instead, one must artificially constrain the displacement corresponding to the shaft whirl mode to stabilize the model against rigid-body displacement. Unfortunately, the whirl displacement component is one of the most significant artifacts of the damage in the real system. In a single-disk model we are limited to analyzing the higher-order harmonic components, which are quite small. In the tests described in Reference 4, it was indeed possible to measure the asymmetric displacement components and to correlate the measured signatures with analytical predictions of the probable damage mode. Thus, there is real evidence that such a measurement is achievable, at least in the setting of a spin pit test.

Additional analyses have been performed using models that depict the stiffness and mass properties of the surrounding system in an approximate way. Figure 7 shows the displacement amplitude associated with a slot bottom crack in one disk, mounted on a shaft with two identical disks, as the shaft stiffness varies. The nominal shaft size J_{nom} corresponds to conditions observed in spin tests of similar components. The far right end of the plot, where the damage-related displacement amplitudes are extremely small, corresponds to a single-disk model. In the one-disk model, the mean and whirl displacements are constrained to eliminate rigid-body motion of the model. For the multiple-disk model on an extremely stiff shaft, damage to a particular disk produces no whirl displacement component because the remainder of the system is so stiff, and the energy penalty associated with any displacement perturbation in the stiffer portion of the system is prohibitively large.

The signatures in Figure 8 correspond to the same system shown in Figure 7, with the shaft size at its nominal value. The characteristic displacement patterns are somewhat more localized, and actually slightly larger in amplitude, than those shown in Figure 6 for the single-disk model.

The upshot of these examples is that the displacements culled from a single-disk model are always artificially small, and the true amplitudes will be a complicated function of the stiffness and mass characteristics of the complete system. Attempts to characterize damage conditions in terms of simplistic concepts like “mass imbalance” fail to acknowledge the complex interactions of all components in the highly-coupled rotordynamic system.

It is also worth mentioning that the presence of other rotating hardware attached to the disk may affect the magnitude and character of disk damage signatures in several ways. The mass of a

disk seal may amount to a significant fraction of the disk weight, thereby affecting the dynamic impedance of the system. If a seal is highly stressed, vibratory motions caused by damage in the seal may dominate the measured signal, making the process of identification more difficult.

Clearly, the issue of whether damage-induced motions can be measured successfully in specific systems remains a pivotal issue, in terms of the role an onboard measurement system might play in monitoring the integrity of the system and providing useful information about remaining life. Further experimental investigation of realistic rotor systems is needed to establish the feasibility of measuring response data with sufficient accuracy for damage mode identification.

6. Signature Filtering and Processing

In this investigation, we assume that a blade tip clearance sensor, such as a capacitance or eddy current probe, is used to collect radial displacement data from the disk. Therefore, the damage modes are characterized by the deviation of the radial displacement from the nominal steady-state value. In the single disk model used for most of the calculations, the first harmonic of the radial displacement, which corresponds to the rigid-body shaft whirl displacement of the disk, is purely an artifact of the model constraints and is filtered out of the results. The procedures we describe for analyzing the measured data are general, and would be identical if the first harmonic components were present.

For both the baseline (known damage) and "measured" cases, we begin by calculating Fourier transforms of the radial displacement data. The displacement amplitude in sector 'i' of the disk can be expressed in the form

$$U_i = U_0 + \sum_{k=1}^{N} A_k \operatorname{Cos}\frac{2\pi k}{N}(i-1) + B_k \operatorname{Sin}\frac{2\pi k}{N}(i-1) \qquad (1)$$

in which A_k and B_k are the Fourier coefficients. The magnitude of the k^{th} harmonic component is $C_k = \sqrt{A_k^2 + B_k^2}$. The *relative* magnitudes of the harmonic components C_k are significant in determining the type of damage mode under consideration, while the absolute magnitudes are important in determining the extent of the damage. The phase differences (related to the ratios A_k/B_k) indicate the location of the damage site around the circumference of the disk.

We first characterize the measured signal by its *direction* in the space of harmonic coordinates (Figure 9). In this step, both the measured signal and baseline damage signatures are normalized

to unit magnitude, and the projection of the measured signal onto each of the reference signatures is computed. The nearest neighbors of the measured signal are selected as candidates for further analysis. It should be noted that Figure 9 is highly simplified, in that the signatures for known cracks of different sizes at a given location do not point in precisely the same direction, but do tend to cluster in a relatively small region of the harmonic space.

For each candidate damage mode, a series of signatures is next extracted from the database for similar cracks of different sizes for use in interpolation. Figure 10 shows a simple example in which the signal amplitudes of bore, hole, and slot bottom cracks of various sizes might be used to estimate crack length for a given signal amplitude. Frequently, and particularly when multiple cracks are present, more than one of these groups might be used to obtain a crack length estimate for a single measured signal. Once the estimated crack length is known, one can interpolate from the corresponding data for stress intensity factors to obtain rough estimates of K and the resulting crack growth per cycle (Figure 11).

7. Damage Identification

Damage estimates have been performed for numerous cases, with the "measured" data being generated using substructured models similar to those used for the baseline analyses. The models used to generate "measured" data contain cracks of different sizes and in different locations from the baseline data, as well as sectors with multiple cracks. Simulated disk measurements have been generated for configurations with single cracks, multiple cracks in a single sector, multiple cracks in different sectors, for crack sizes different from those in the database of known damage conditions.

Crack length estimates based on selection of the single damage mode closest to the measured signal in harmonic space ("nearest neighbor") are shown in Figure 12. Notice that the crack length estimates are quite accurate, but in some cases the estimates are non-conservative. The reason for this is that some estimates, especially for multiply-cracked disks, will have been based on crack types or locations that are not correct. Using several near-neighbor signatures to make multiple estimates does result in conservative predictions, as shown in Figure 13. In practice, one would expect to augment the database of known damage conditions as time progresses, allowing the predictions to converge on the correct mode of damage after several successive measurements. A second benefit of this approach is that the tolerances applied to select the

specific signatures to be used for damage estimates almost certainly can be reduced as more damage conditions are added to the database, giving a sharper estimate of the mode and extent of damage associated with the dominant defect.

8. Prediction of Remaining Fatigue Life

Given a reasonable body of fatigue performance data for the material(s) of interest, useful estimates may be made for the probable crack growth rate and remaining fatigue life of the component of interest. In the examples below, we analyze the same disk model described in section 3, operating at 18,000 RPM, with stress ratio R = 0.10.

To obtain a more accurate relationship between crack size and stress intensity for use in the life prediction, a series of 16 models has been analyzed for each crack configuration for crack lengths between 0.125 mm and 3.75 mm. In each case, a cubic polynomial fit is used to describe the ΔK-a relationship (Figure 14). For simplicity, we will use a single material, temperature, and R-ratio, with the crack growth rate and stress intensity range related by[18]

$$\frac{da}{dN} = 5.0 \times 10^{-11}\, \Delta K^{3.70} \tag{2}$$

Here the stress intensity range has units of MPa√m, and the crack growth rate is in mm/cycle.

One obvious approach to combining the ΔK-a and crack growth rate data is to isolate dN in Eq. 2 and integrate,

$$N = \int_0^a \frac{da}{C\,\Delta K^n} \tag{3}$$

giving a relationship between crack length and number of cycles. The relation in Eq. 3 assumes an initiation life of zero cycles. A similar but more useful form of this relationship is obtained by integrating between the current crack length (as estimated from the signal analysis) and the critical crack length,

$$N_{REM} = \int_a^{a_c} \frac{da}{C\,\Delta K^n} \tag{4}$$

Eq. 4 gives the estimated remaining fatigue crack growth life directly based on the current estimate of crack length (Figure 15).

9. Summary and Conclusions

A substructure-based analytical testbed has been created to study the problem of identification of cracking damage in turbine engine disks. The substructuring approach makes it relatively simple to model the damaged regions in detail, thereby allowing estimates not only of crack location and size, but also of stress intensity factors and likely crack growth rates. Identification of the damage modes in a measured signal is accomplished by analyzing the Fourier-transformed signature and that of several known damage modes residing in a database for the component of interest. The direction of the transformed signal in harmonic space indicates the probable type and location of the crack; using known signatures for cracks of the same type, estimates of the crack size are obtained through interpolations based on the amplitude of the measured signal.

A particularly important use of the present methodology is in refining one's estimate of the type, location, and extent of damage as data become available at successively later times. In the process, additional relevant damage modes for the component can be analyzed and added to the database, as needed, to help sharpen the estimation of the probable damaged condition.

Further analyses of multiple-disk systems, as well as experimental investigations, are needed to establish the feasibility of measuring displacement data to the accuracy required for reliable assessment of damage evolution in engine disks. The consideration of blade vibrations is a further area of interest because of the rich harmonic content that is introduced into the measured data. Depending on the characteristics of particular systems, it may be possible to monitor disk damage, blade damage, or both from a given type of motion sensor. The feasibility of each of these options must be assessed to define a logical approach for managing the remaining life of the complete system.

Acknowledgement

This work was performed at the Air Force Research Laboratory, Materials and Manufacturing Directorate, AFRL/RXLMN, Wright-Patterson Air Force Base, OH, USA, under on-site Contract No. FA8650-04-C-5200. The authors gratefully acknowledge the support of Dr. Leo Christodoulou of the Defense Advanced Research Projects Agency (DARPA) under DARPA order S271 and Dr. Victor Giurgiutiu of the Air Force Office of Scientific Research (AFOSR) under task 2306-6M2AL8.

References

1. Larsen, J.M. and Christodoulou, L., Integrating damage state awareness and mechanism-based prediction, *J. Materials*, March 2004, **56**, (3) p. 14.

2. Christodoulou, L. and Larsen, J.M., Using materials prognosis to maximize the utilization potential of complex mechanical systems, *J. Materials*, March 2004, **56**, (3), pp. 15-19.

3. G. J. Kacprzynski, A. Sarlashkar, M. J. Roemer, A. Hess, and W. Hardman, Predicting Remaining Life by Fusing the Physics of Failure Modeling with Diagnostics, *J. Materials*, March 2004, **56**, (3), pp. 29-35.

4. von Flotow, A., Tappert, P., Mercadal, M. and Hardman, W., Successes and failures for LCF rotor burst prognosis using blade tip sensors, Paper GT-2004-54131, *Proc. ASME Turbo Expo 2004*, Vienna, Austria, June 2004.

5. Russ, S.M., Rosenberger, A.H., Larsen, J.M., Berkeley, R.B., Carroll, D., Cowles, B.A., Holmes, R.A., Littles, J.W. Jr., Pettit, R.G. and Schirra, J.J., Demonstration of advanced life-prediction and state-awareness technologies necessary for prognosis of turbine engine disks, in *Health Monitoring and Smart Nondestructive Evaluation of Structural and Biological Systems III*, Proc. SPIE Conference on Smart Structures and Materials NDE for Health Monitoring and Diagnostics, San Diego, California, March 2004.

6. Ko, J.M. and Ni, Y.Q., Technology developments in structural health monitoring of large-scale bridges, *Engineering Structures*, October 2005, **27** (12), pp. 1715-1725.

7. Chang, P.C., Flatau, A., and Liu, S.C., Review paper: health monitoring of civil infrastructure, *Structural Health Monitoring*, September 2003, **2** (3), pp. 257-267.

8. Giurgiutiu, V., Zagrai, A.N. and Bao, J., Piezoelectric wafer embedded active sensors for aging aircraft structural health monitoring, *Structural Health Monitoring*, July 2002, **1** (1), pp. 41-61.

9. Takeda, N., Tajima, N., Sakurai, T., and Kishi, T., Recent advances in composite fuselage demonstration program for damage and health monitoring in Japan, *Structural Control and Health Monitoring*, December 2005, **12** (3-4), pp. 245-255.

10. Saavedra, P.N., and Cuitiño, L.A., Vibration analysis of rotor for crack identification, *J. Vib. and Control*, 2002, **8**, pp. 51-67.

11. Gasch, R., A survey of the dynamic behavior of a simple rotating shaft with a transverse crack, *J. Sound Vib.*, 1193, **160** (2), pp. 313-332.

12. He, Y., Guo, D., and Chu, F., Using genetic algorithms and finite element methods to detect shaft crack for rotor-bearing system, *Math. Comp. Simulation*, 2001, **57**, pp. 95-108.

13. Gounaris, G.D. and Papadopoulos, C., Crack identification in rotating shafts by coupled response measurements, *Eng. Frac. Mech.*, 2002, **69**, pp, 339-352.

14. Seker, S., Ayaz, E., and Türkcan, E., Elman's recurrent neural network applications to condition monitoring in nuclear power plane and rotating machinery, *Eng. Appl. Art. Intelligence*, 2003, **16**, pp. 647-656.

15. Seibold, S. and Weinert, K., A time domain method for the localization of cracks in rotors, *J. Sound Vib.*, 1996, **195**, (1), pp. 57-73.

16. _____, *Zencrack User's Manual, Version 7.1*, Zentech International, Ltd., Camberley, Surrey, UK, September 2003.

17. _____, *ABAQUS Analysis User's Manual, Version 6.7*, Dassault Systèmes, Providence, Rhode Island, USA, 2007.

18. Luo, J. and Bowen, P., Small and long fatigue crack growth behavior of a PM Ni-based superalloy, Udimet 720, *Int. J. Fatigue*, 2004, **26** (2), pp. 113-124.

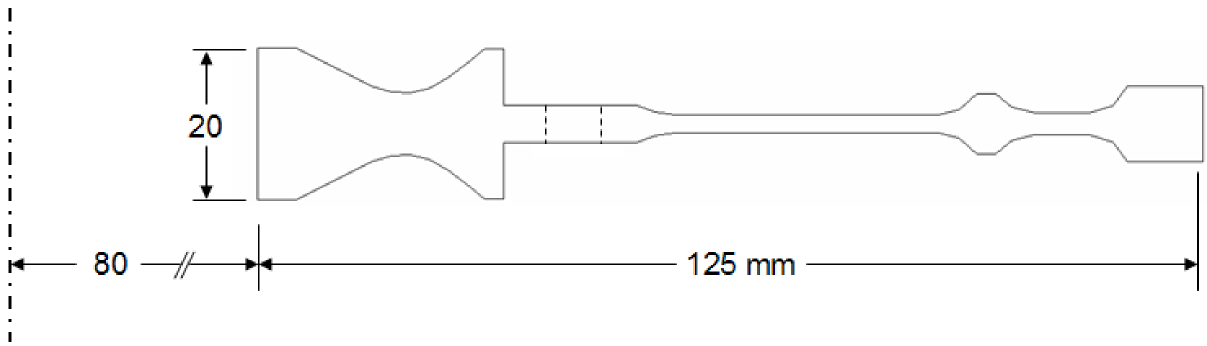

Figure 1. Generic Disk Model Cross Section.

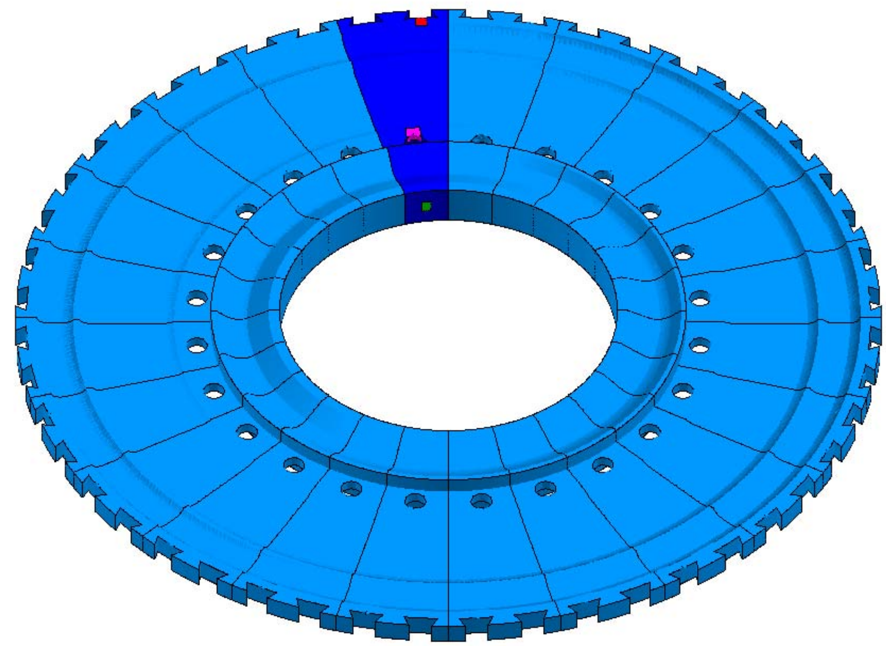

Figure 2. Substructured Generic Disk Model.

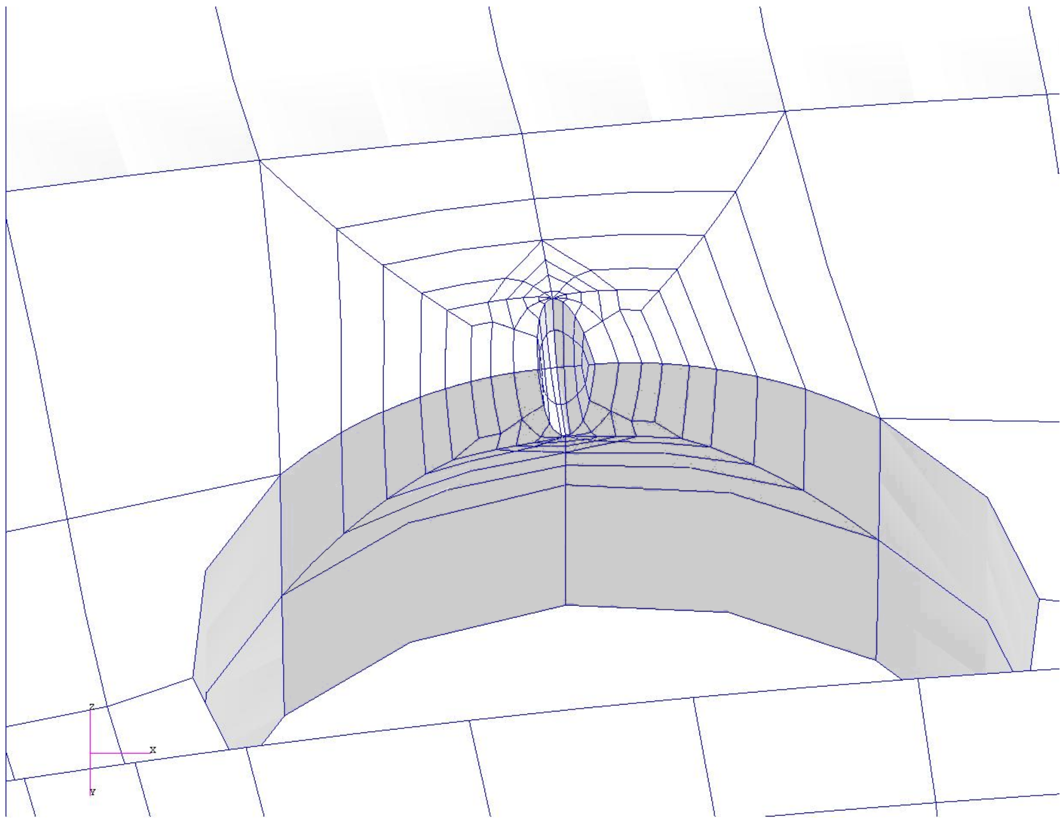

Figure 3. Detail of Deformed Crack Mesh near Hole Edge.

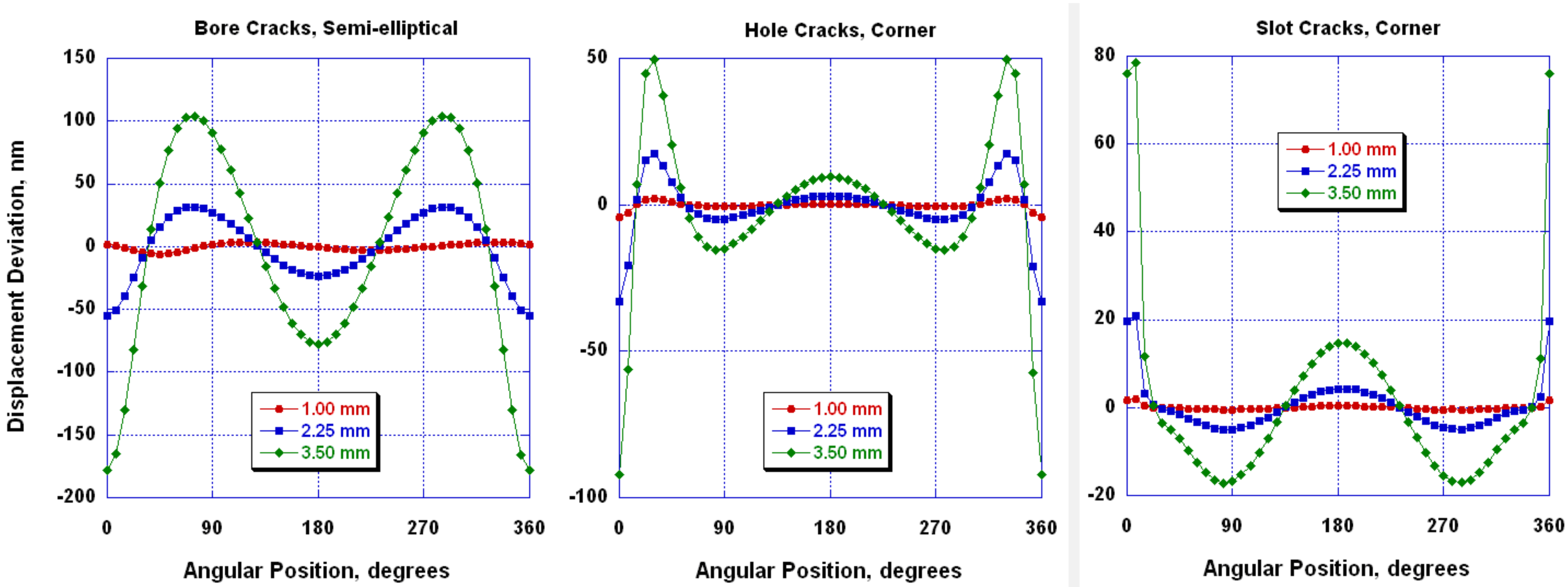

Figure 4. Baseline Signatures for Radial Displacements in Known Crack Configurations: (a) Bore; (b) Web Hole; (c) Blade Slot.

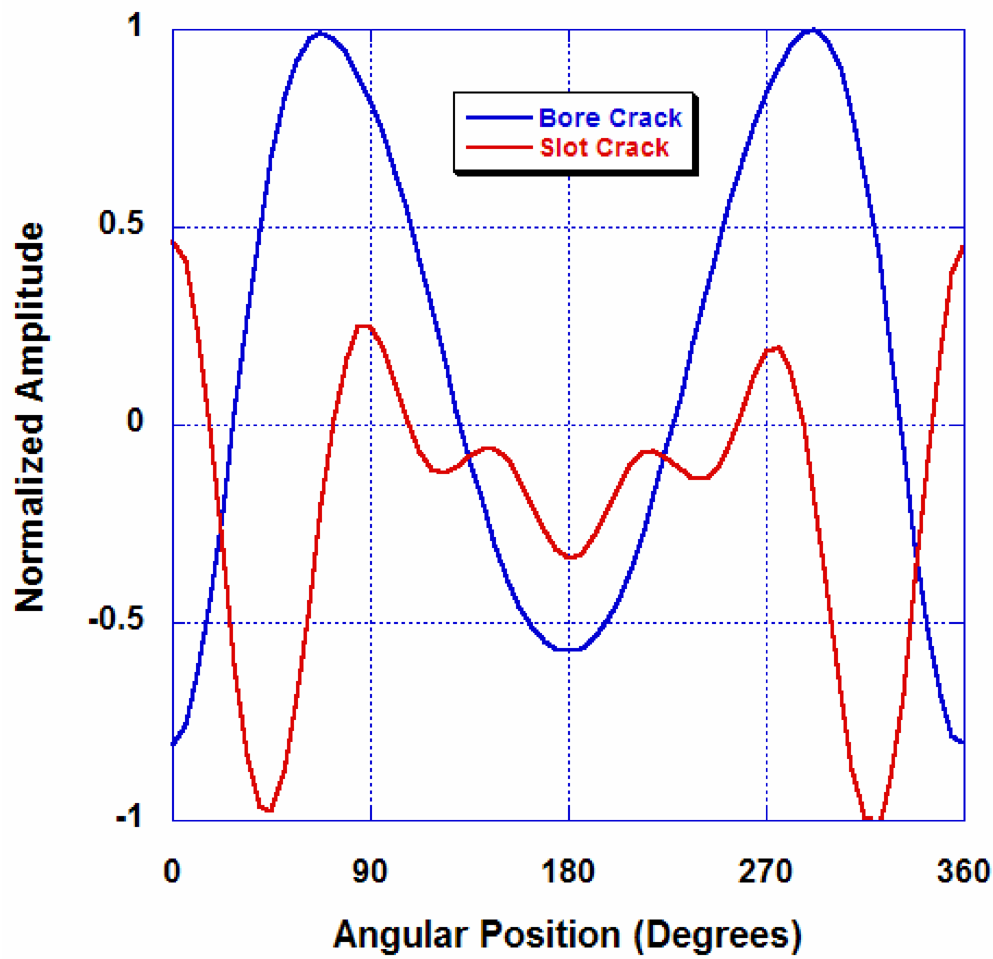

Figure 5. Displacement Amplitudes from Model of Fielded Disk.

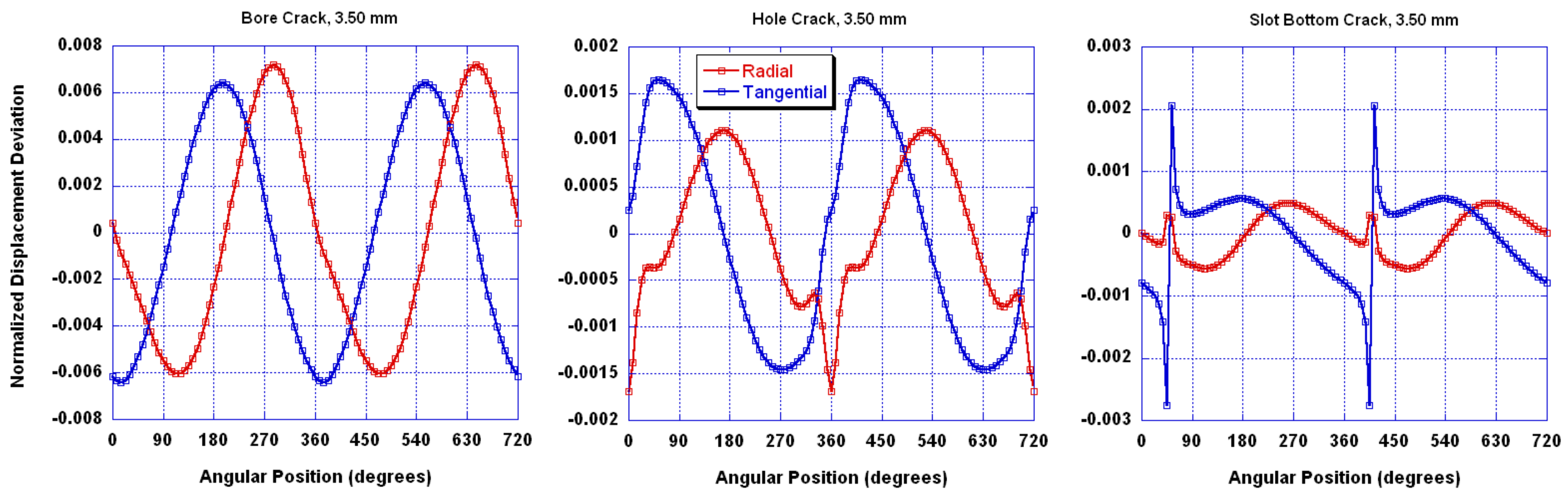

Figure 6. Comparison of Radial and Tangential Displacement Signatures for Various Crack Locations in a Single Disk.

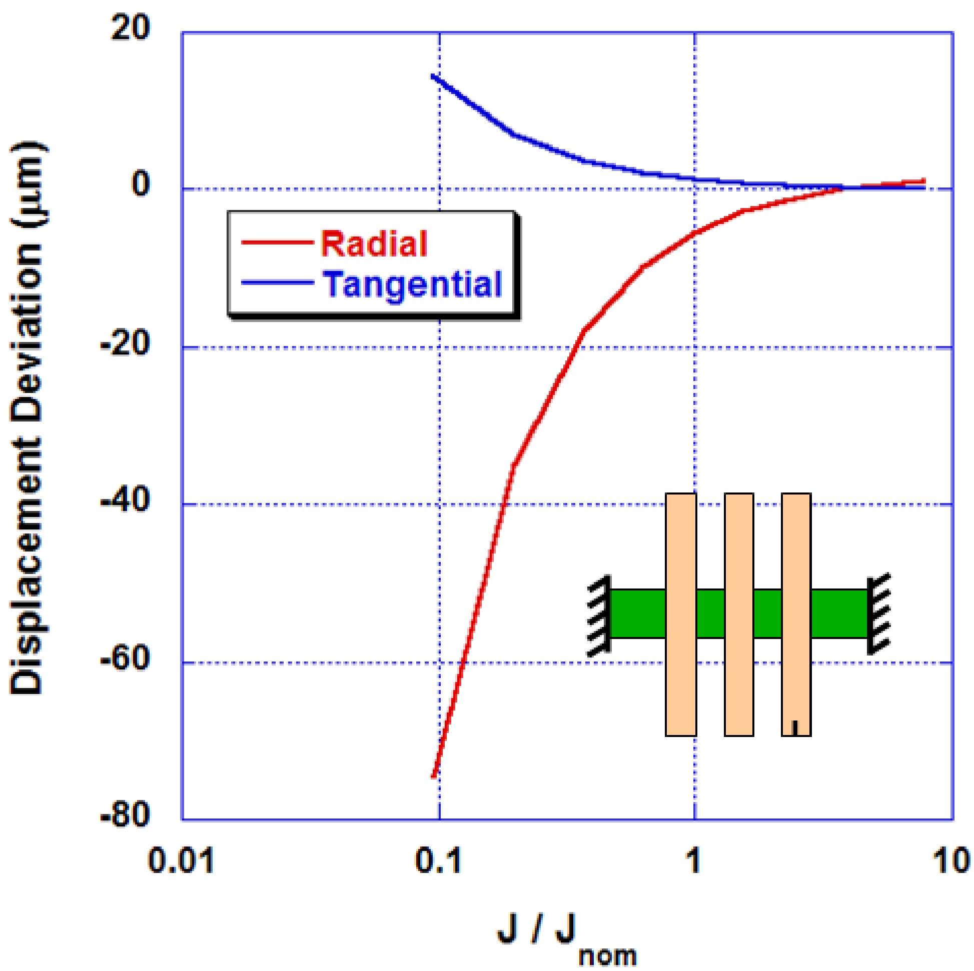

Figure 7. Displacement Amplitude Variation with Shaft Stiffness.

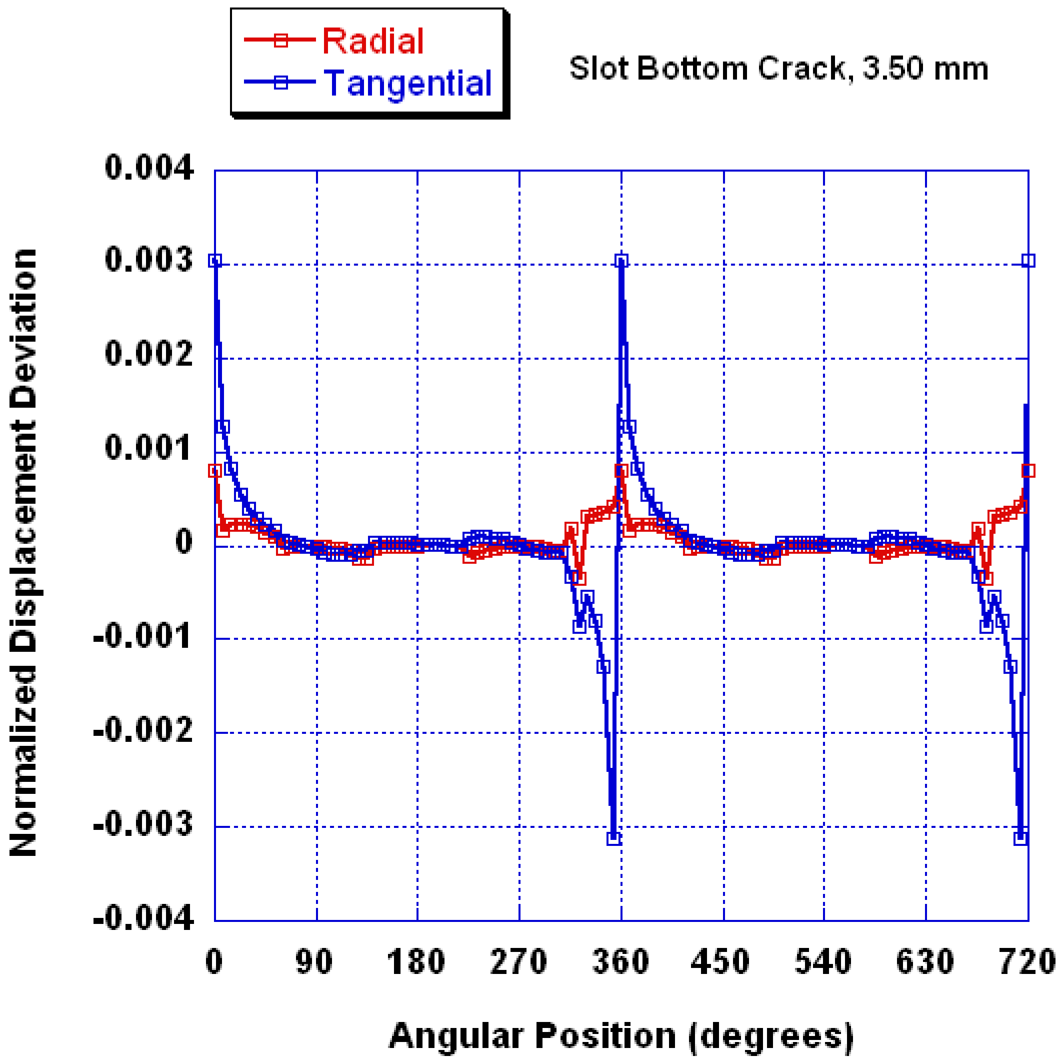

Figure 8. Displacement Signatures due to Damage in Neighboring Disks.

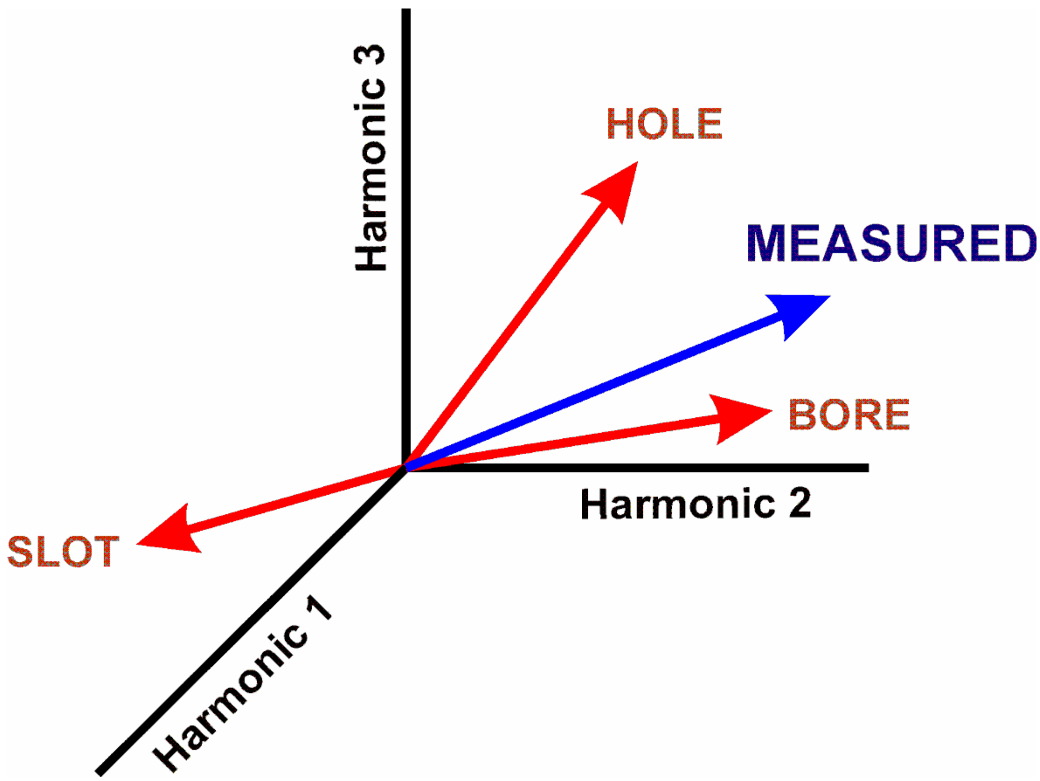

Figure 9. Signature Patterns in Harmonic Coordinate Space.

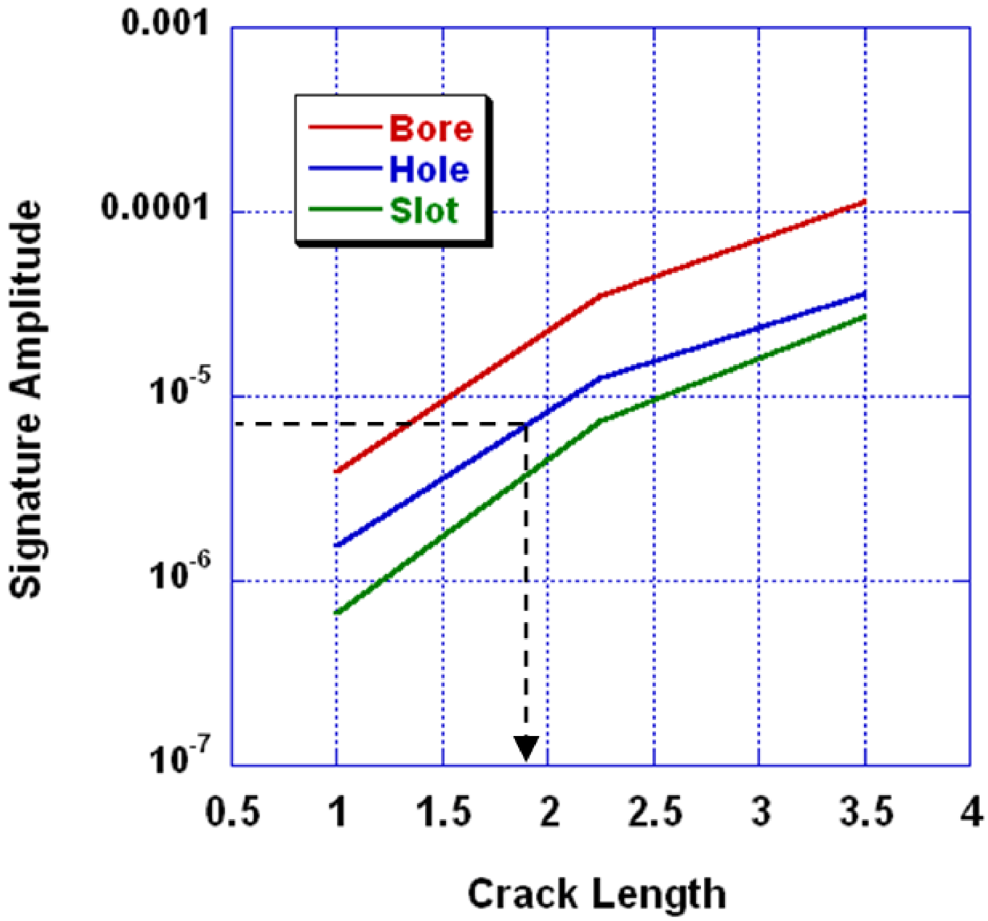

Figure 10. Inverse Interpolation for Estimated Crack Length.

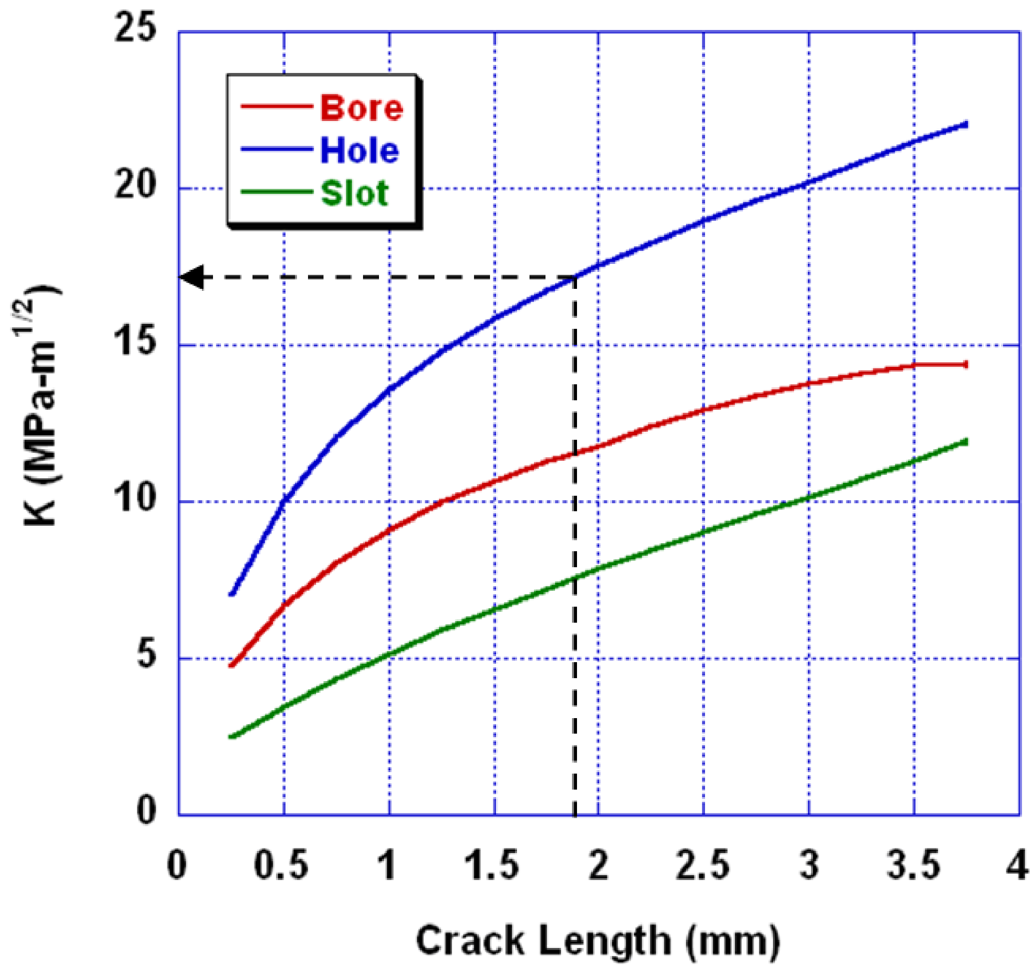

Figure 11. Stress Intensity Factor Estimate from Crack Length.

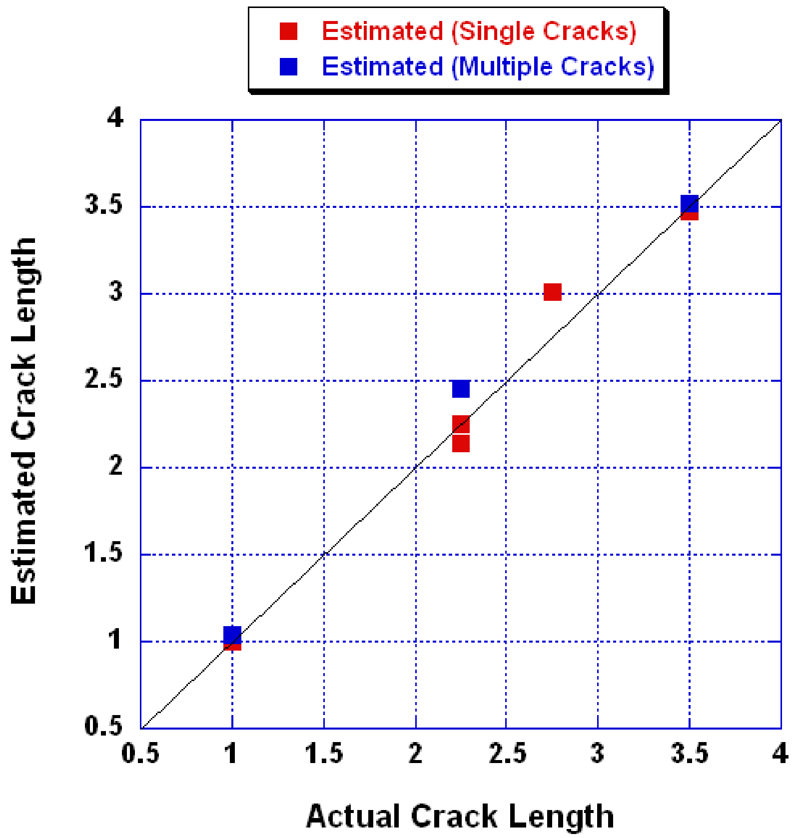

Figure 12. Crack Length Estimates from Nearest Neighbors in Harmonic Coordinate Space.

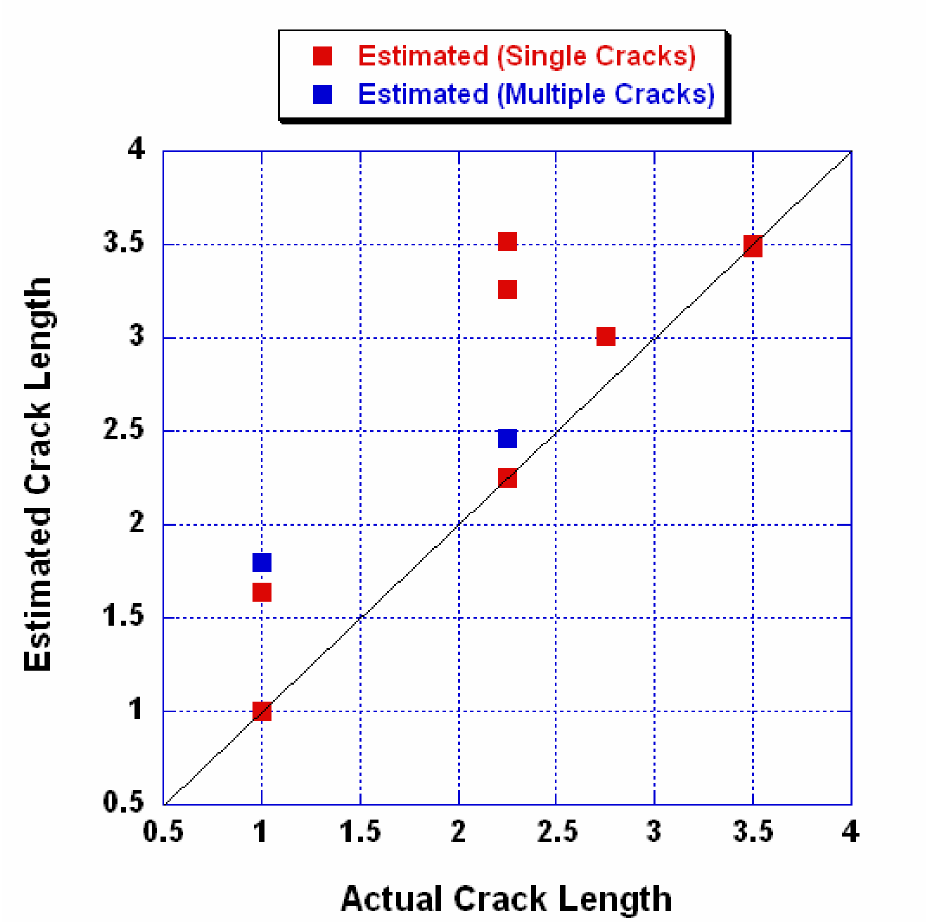

Figure 13. Crack Length Estimates based on Multiple Neighbors in Harmonic Coordinate Space.

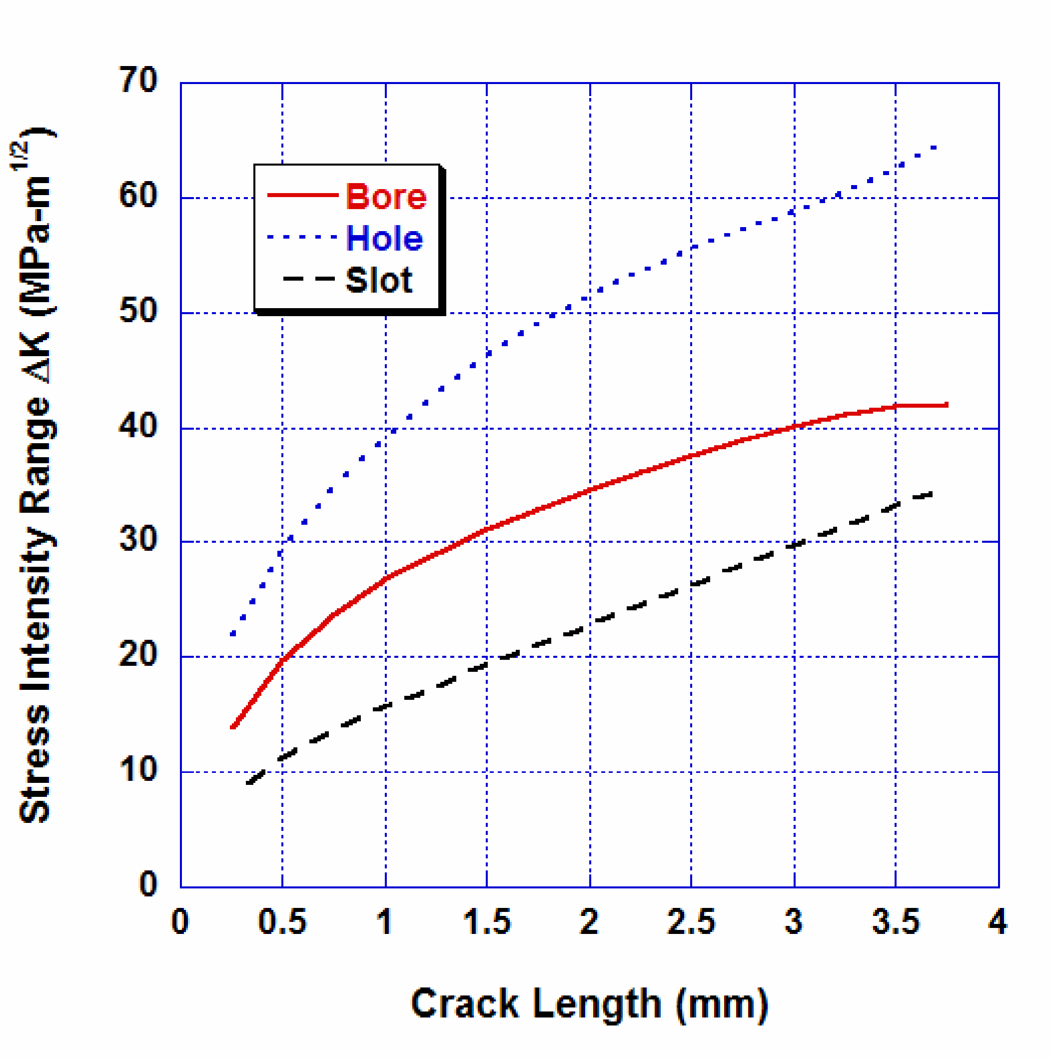

Figure 14. Polynomial Fits for ΔK as a Function of Crack Length.

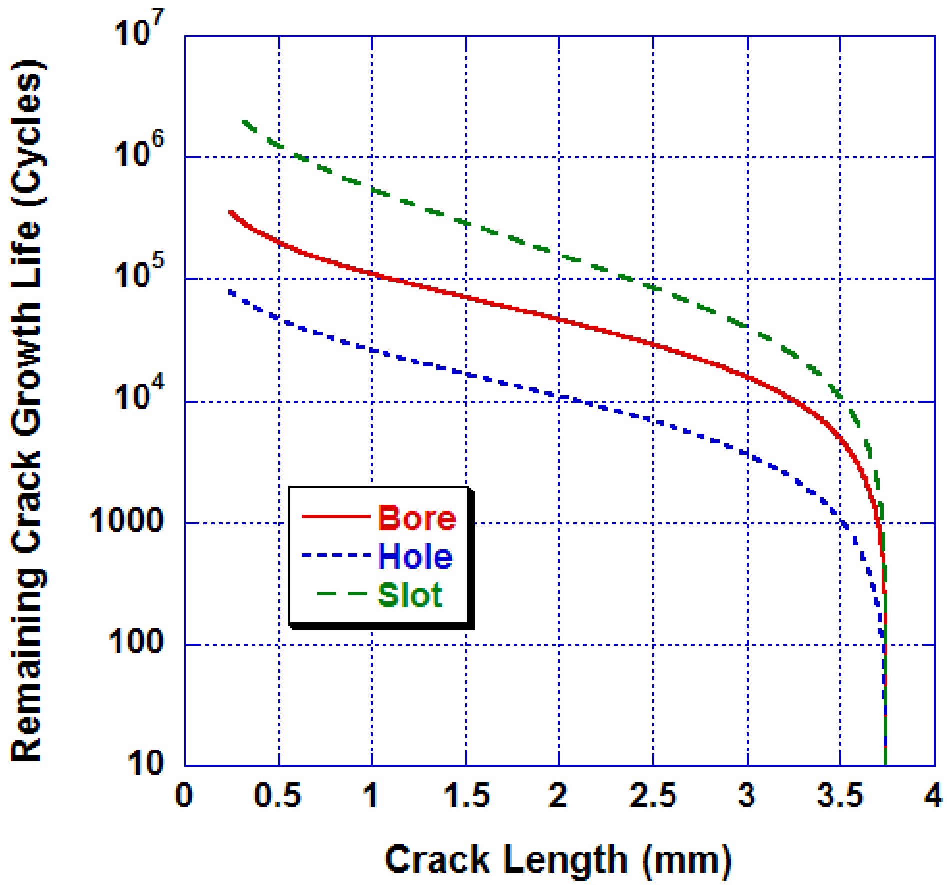

Figure 15. Remaining Life as a Function of Crack Length.